Received: 20 April 2017 | Revised: 21 September 2017 | Accepted: 15 October 2017

DOI: 10.1111/ajt.14547

ORIGINAL ARTICLE

AJT

Immunoisolation of murine islet allografts in vascularized sites through conformal coating with polyethylene glycol

Vita Manzoli[1,2] | Chiara Villa[1,3] | Allison L. Bayer[1,4] | Laura C. Morales[1] | R. Damaris Molano[1] | Yvan Torrente[3] | Camillo Ricordi[1,4,5,6,7] | Jeffrey A. Hubbell[8] | Alice A. Tomei[1,6,7]

[1]Diabetes Research Institute, University of Miami Miller School of Medicine, Miami, FL, USA

[2]Department of Electronics, Information and Bioengineering , Politecnico di Milano, Milano, Italy

[3]Stem Cell Laboratory, Department of Pathophysiology and Transplantation, Universitá degli Studi di Milano, Unit of Neurology, Fondazione IRCCS Ca' Granda Ospedale Maggiore Policlinico, Centro Dino Ferrari, Milan, Italy

[4]Department of Microbiology and Immunology, University of Miami Miller School of Medicine, Miami, FL, USA

[5]Department of Medicine, University of Miami Miller School of Medicine, Miami, FL, USA

[6]Department of Surgery, University of Miami Miller School of Medicine, Miami, FL, USA

[7]Department of Biomedical Engineering, University of Miami, Miami, FL, USA

[8]Department of Molecular Engineering, University of Chicago, Chicago, IL, USA

Correspondence
Alice A. Tomei
Email: atomei@miami.edu

Funding information
Fondazione Tronchetti Provera; Diabetes Research Institute Foundation; National Institutes of Health (NIH), Grant/Award Number: DK109929; Fondazione IRCCS Ca' Granda Ospedale Maggiore Policlinico; Juvenile Diabetes Research Foundation International, Grant/Award Number: 17-2001-268, 17-2010-5, 17-2012-361

Islet encapsulation may allow transplantation without immunosuppression, but thus far islets in large microcapsules transplanted in the peritoneal cavity have failed to reverse diabetes in humans. We showed that islet transplantation in confined well-vascularized sites like the epididymal fat pad (EFP) improved graft outcomes, but only conformal coated (CC) islets can be implanted in these sites in curative doses. Here, we showed that CC using polyethylene glycol (PEG) and alginate (ALG) was not immunoisolating because of its high permselectivity and strong allogeneic T cell responses. We refined the CC composition and explored PEG and islet-like extracellular matrix (Matrigel; MG) islet encapsulation (PEG MG) to improve capsule immunoisolation by decreasing its permselectivity and immunogenicity while allowing physiological islet function. Although the efficiency of diabetes reversal of allogeneic but not syngeneic CC islets was lower than that of naked islets, we showed that CC (PEG MG) islets from fully MHC-mismatched Balb/c mice supported long-term (>100 days) survival after transplantation into diabetic C57BL/6 recipients in the EFP site (750-1000 islet equivalents/mouse) in the absence of immunosuppression. Lack of immune cell penetration and T cell allogeneic priming was observed. These studies support the use of CC (PEG MG) for islet encapsulation and transplantation in clinically relevant sites without chronic immunosuppression.

KEYWORDS
animal models: murine, basic (laboratory) research/science, bioengineering, diabetes, encapsulation, islet transplantation, islets of Langerhans, regenerative medicine, translational research/science

Abbreviations: ALG, alginate; BL, blood; CC, conformal coated; DTT, dithiothreitol; dVS, divinyl sulfone; ECM, extracellular matrix; EFP, epididymal ft pad; GSIR, glucose-stimulated insulin release; H&E, hematoxilin & eosin; IFNgamma, interferon gamma; IP, intraperitoneal cavity; KD, kidney subcapsular space; MAL, maleimide; MG, Matrigel; MLR, mixed lymphocyte reaction; mTOR, mechanistic target of rapamycin; OCR, oxygen consumption rate; PBL, peripheral blood lymphocyte; PEG, polyethylene glycol; R, responders; ROS, reactive oxygen species; S, stimulators; SC, subcutaneous; SD, standard deviation; SPL, spleen; T1D, type 1 diabetes.

1 | INTRODUCTION

Islet transplantation can restore glucose homeostasis and prevent complications of type 1 diabetes (T1D).[1] Despite recent clinical success, the applicability of islet transplantation is limited by the need for chronic immunosuppression to inhibit undesired allogeneic and recurrent autoreactive immune responses against transplanted islets. Moreover, the use of chronic immunosuppression is the main cause of adverse events in islet transplantation,[2-4] resulting in islet transplantation offered only in the most severe cases of T1D. There is a strong need to develop novel strategies that would eliminate the need for chronic immunosuppression and make islet transplantation a viable option for patients with T1D. Islet encapsulation could allow transplantation without the need for chronic immunosuppression, thereby extending the procedure to a larger number of patients, including children.[5-7] Despite promising results with many different microencapsulation strategies showing protection to allogeneic and xenogeneic islets after transplantation without systemic immune suppression in mice,[8,9] clinical trials have only proven safety, not long-term efficacy.[10-12] The majority of human trials have been conducted in the peritoneal cavity (intraperitoneal, IP) with capsules of uniform and large diameter (500-1500 μm, despite islets having a variable size between 50 and 350 μm). Clinical failure of those traditional encapsulation protocols may be associated with 2 critical factors: (1) transplant site and (2) capsule size. Islet central hypoxia is one of the main determinants of graft outcomes.[8] Minimizing hypoxia by islet transplantation in well-vascularized sites and/or by minimizing capsule thickness may lead to better outcomes. We previously demonstrated that transplantation of encapsulated islets in confined and vascularized sites like the epididymal fat pad (EFP) improves the outcome of naked[13] and encapsulated islet grafts[14] in mice. However, curative doses of islets encapsulated in traditional capsules add up to hundreds of milliliters and cannot be transplanted in these confined sites, as they can accommodate only a few milliliters grafts.

We recently developed a method for coating islets with a uniformly thin hydrogel layer that conforms to the islet shape and that is independent of islet size: *conformal coating*.[15] Because the volume of conformal coated (CC) islet grafts is comparable to the volume of naked islets grafts, CC islets can be transplanted in confined well-vascularized sites in curative doses. We previously reported the design of the encapsulation device and of the CC hydrogels[15] using polyethylene glycol (PEG) because of its greater physicochemical stability compared to other encapsulation materials.[14] We showed that PEG functionalized with divinyl sulfone (PEG-dVS) and crosslinked with dithiothreitol (DTT) needed to be supplemented with a viscosity enhancer to allow formation of conformal coatings and for modulating the coating permeability, which is critical for CC islet functionality.[15] By using alginate (ALG) as a viscosity enhancer for PEG hydrogels for coatings we showed physiological glucose-stimulated insulin release (GSIR) from CC islets in vitro. Our previous work showed sustained graft viability and function for >100 days in vivo in syngeneic murine islet transplant models in the nonclinically applicable but commonly evaluated kidney subcapsular space (KD).[15] This CC platform has laid the groundwork for a novel approach to minimizing the capsule thickness and volume of encapsulated islet grafts through conformal coating, but has not been explored in allogeneic islet transplantation in clinically relevant sites without immunosuppression.

Here we have built on these results and refined the composition of conformal coatings to provide immunoisolation properties to CC islets in fully MHC-mismatched diabetic mice without any immunosuppression and in clinically applicable confined and well-vascularized sites.

2 | MATERIALS AND METHODS

2.1 | Islet isolation and culture, diabetes induction, and islet transplantation

Pancreatic islets were isolated and cultured as described previously.[15] Diabetes was induced in mice by administration of intravenous streptozotocin. Isolated islets were then transplanted under the kidney capsule (KD) or in the epididymal fat pad (EFP) of diabetic mice, as described elsewhere.[14,15]

2.2 | Encapsulation materials and methods

For encapsulations, 10% w/v 10 kDa 8-arm PEG (either dVS or maleimide [MAL], JenKem Technologies) with 1.6% UP-MVG (Novamatrix) alginate solution (PEG ALG) or with Matrigel (MG, Corning) (PEG MG) was cross-linked with DTT (Calbiochem) at a 1:4 molar ratio. Pancreatic islets were resuspended in the PEG ALG DTT or PEG MG DTT solution at a 50,000 islet equivalents (IEQ)/ml concentration and conformal coated or digested with "enzyme" to obtain graft-associated immune cells for FACS analysis as described previously.[15]

2.3 | Viability/functionality assays in vitro

Islet viability and oxygen consumption rate (OCR) measurement [14] GSIR and perfusion were performed as described previously.[15]

2.4 | Evaluation of capsule completeness and permeability

For completeness assessment, 2000 kDa FITC-Dextran (Sigma) was added to the hydrogel solution used for encapsulation or to CC media. In addition, capsules were stained with anti-PEG antibody. Samples were imaged using a Leica SP5 confocal microscope. Permeability of CC hydrogels to FITC-Dextran of selected molecular weight was measured as described previously.[15]

2.5 | Cytokine production of CC islets

CC (PEG MG) and naked islets were cultured for 1, 2, 7, and 14 days after encapsulation and Multiplex Immunoassay (Affymetrix) was performed on the supernatants.

2.6 | Evaluation of CC capsules and explanted grafts by histology and flow cytometry

Explanted grafts were either fixed in formalin, paraffin embedded and thin-sectioned, or digested.[16] Hematoxylin and eosin (H&E)

staining and immunostaining/imaging using a Leica SP5 confocal microscope was done using anti-PEG (Abcam), Hoechst (Molecular Probes), glucagon (Biogenex), insulin (Dako), Mac2 (Cedarlane), CD31 (Abcam), CD3 (Cell Marque), CD45 (BD Biosciences), and B220 (eBioscience). For flow cytometry, cells were stained with live/dead (Invitrogen), CD3, CD8, CD44, CD62L, CD25, CD127, Ki-67, B220, CD45 (BD Bioscience), CD4, FoxP3, B220, F4/80, I-A/I-E, GR-1, CD11c, and CD11b (eBioscience), and 150 μL samples (total volume of each well) acquired on a CytoFLEX.

2.7 | Alloresponse monitoring in islet graft recipients by ex vivo mixed lymphocyte reaction (MLR)

Peripheral blood lymphocytes (PBLs) were isolated from B6 recipient of CC (PEG ALG), CC (PEG MG), naked Balb/c islets, or islet-free fibrin scaffolds 14 days after transplantation, labeled with cell trace (Responders: R) and co-cultured with PBL (BL) or splenocytes (SPLs) from naive Balb/c mice (Stimulators: S). Four days after, culture wells were stained and acquired on a CytoFLEX.

2.8 | Statistical analysis

Prism 6 was used for all data analysis. Data are presented as mean ± standard deviation (SD). Statistical analysis was performed as previously described.[14]

3 | RESULTS

3.1 | Conformal coating using PEG-dVS ALG hydrogels does not provide immunoisolation to rodent islets

Following promising results of CC using PEG ALG hydrogels in syngeneic islet transplant models at the KD site in mice, we investigated whether CC with PEG ALG provided immunoisolation to fully MHC-mismatched islet allografts. Two days after coating, we transplanted CC (PEG ALG) or naked Balb/c islets (Figure 1A) at the KD site of diabetic B6 mice (1000 IEQ/mouse). Unlike naked islets, which reversed diabetes and were then rejected (13-20 days), CC (PEG ALG islets) never reversed diabetes (Figure 1B). Analysis of islet viability (Figure 1C) and GSIR function (Figure 1D) at the time of transplantation showed no significant difference between the naked and the CC (PEG ALG) islets, suggesting that failure of CC (PEG ALG) islets to reverse diabetes was not due to poor viability or lack of functionality of CC Balb/c islets prior to transplantation. However, histological analysis of the CC (PEG ALG)– retrieved grafts showed only a few insulin-positive islets remaining at the graft site, with most capsules lacking any residual islets (Figure 1E-F), suggesting that CC islets were rejected after transplantation. Furthermore, unlike what we had observed previously for syngeneic CC grafts,[15] we found that macrophages were present on the majority of the capsule surface (Figure 1G), suggesting that host responses to CC allografts mediated graft loss. To address this poor immunoisolation and biocompatibility of PEG ALG CC allogeneic islets in the KD site of diabetic B6 mice, we evaluated engraftment of encapsulated islet allografts in well-vascularized sites[14] by implanting CC (PEG ALG) Balb/c islets in the EFP of diabetic B6 mice (Figure 1H). We found that CC (PEG ALG) islets transplanted in the EFP site reversed diabetes, unlike islets transplanted in the KD site, but were rejected at rates comparable to that of the naked islets (Figure 1I). Histological analysis of CC (PEG ALG) grafts 4 days after implantation in the EFP site confirmed cell infiltrates (Figure 1J, H&E staining). Immune cell recruitment to the graft was observed (Figure 1K, CD45 staining), including T and B cells (Figure 1L, CD3 and B220 staining) and macrophages (Figure 1M, MAC2 staining) infiltration through the CC (PEG ALG) capsules, which could be mediating rejection of the CC grafts.

To further confirm that the mechanisms of CC graft loss was dependent on poor immunoisolation of PEG ALG hydrogels, we investigated the barrier properties of CC (PEG ALG) membranes to large (2000 kDa) FITC-labeled dextran, either entrapped within coating hydrogels (Figure 1N) or added to the CC media (Figure 1O). We found that coatings presented a microporous structure, further supporting that lack of immunoisolation of CC (PEG ALG) hydrogels was an underlying mechanism for the failure of CC (PEG ALG) islet allografts. Therefore, we focused on refining the composition of CC capsules to improve immunoisolation of CC capsules and allow long-term allograft functionality in mice.

3.2 | Refining the composition of CC hydrogels to improve immunoisolation

First, to develop a better strategy for CC in the transplant setting, we wanted to assess whether suboptimal biocompatibility of PEG ALG at the KD site, in addition to poor immunoisolation, was also contributing to the failure of CC (PEG ALG) allografts to reverse diabetes. We compared the host reactivity to control PEG-dVS capsules in the subcutaneous (SC), KD, and EFP site. We found that reactivity to PEG gels in the EFP site was lower (higher biocompatibility) than in the KD capsule and in the SC site as assessed by H&E staining showing fibrotic cell layers (Figure 2A). Given the reactivity of empty PEG-dVS capsules, we next tested PEG functionalized with MAL, a more stable functional group that reacts with DTT to form hydrogels by a Michael type addition.[17] We found that PEG-MAL biocompatibility was higher than PEG-dVS in both the KD and SC sites (Figure 2B). Despite different coating biocompatibility, CC (PEG-dVS) and CC (PEG-MAL) islets displayed comparable viability (Figure 2C) and GSIR (Figure 2D) in vitro. Therefore, we selected PEG-MAL as coating composition for the studies that followed.

Next, we wanted to test a more biologically relevant material than ALG as a viscosity enhancer and additive for PEG-MAL hydrogels to improve the immunoisolating properties of CC. Because of the natural composition of islet-like extracellular matrix (ECM) and its role in preventing leukocyte infiltration of pancreatic islets in the native pancreas,[18] we replaced ALG with a commercially available reagent, Matrigel (or MG), which resembles the composition of islet ECM. We found that the MG addition to PEG-MAL (PEG) conferred the desired rheological properties to PEG pregels.[15] This allowed generation of 40-mm thick (Figure 2E)

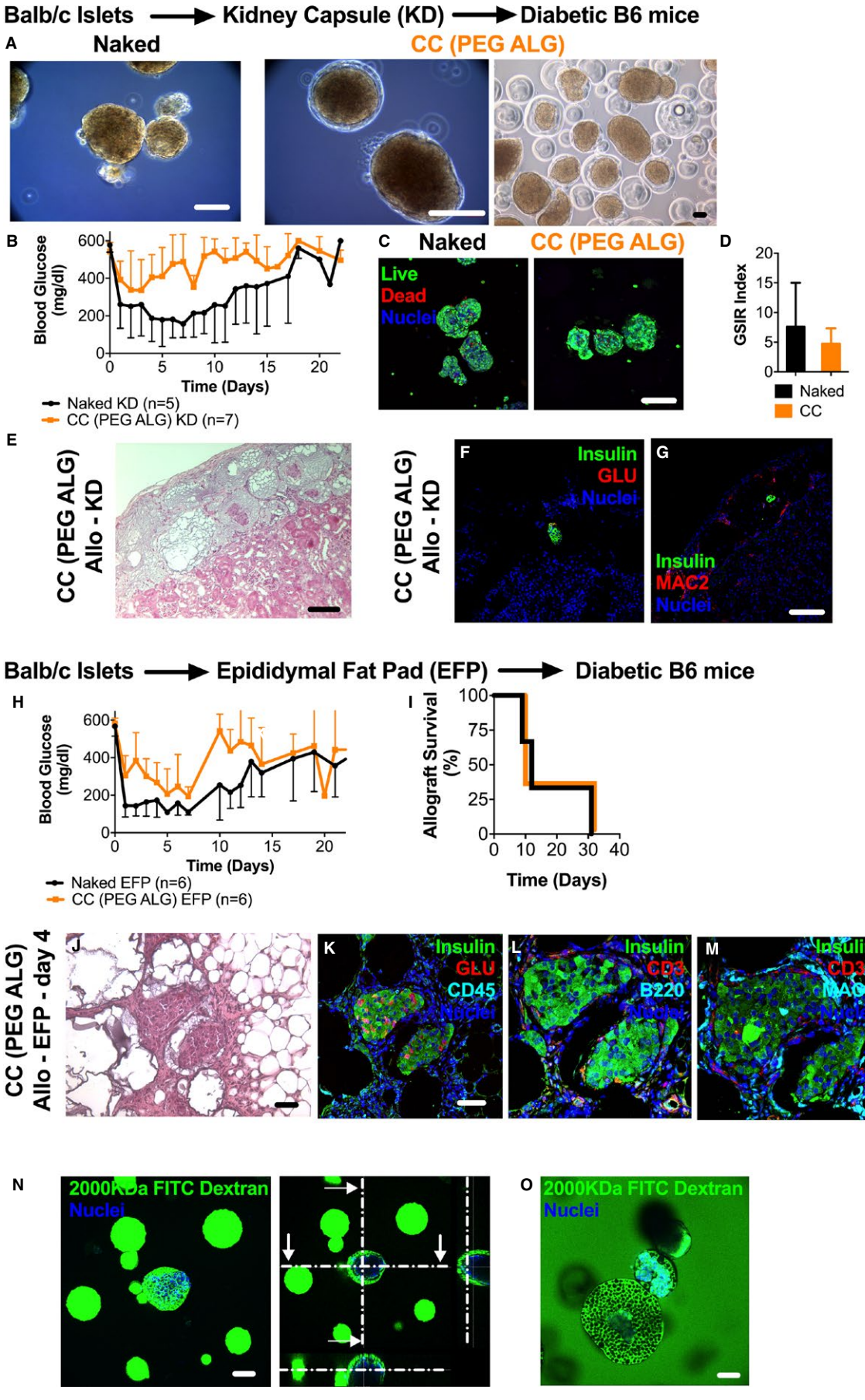
Balb/c Islets → Kidney Capsule (KD) → Diabetic B6 mice
A
Naked
CC (PEG ALG)
B
Blood Glucose (mg/dl)
Time (Days)
Naked KD (n=5)
CC (PEG ALG) KD (n=7)
C
Naked
CC (PEG ALG)
Live
Dead
Nuclei
D
GSIR Index
Naked
CC
E
CC (PEG ALG) Allo - KD
F
Insulin
GLU
Nuclei
G
Insulin
MAC2
Nuclei
Balb/c Islets → Epididymal Fat Pad (EFP) → Diabetic B6 mice
H
Blood Glucose (mg/dl)
Time (Days)
Naked EFP (n=6)
CC (PEG ALG) EFP (n=6)
I
Allograft Survival (%)
Time (Days)
CC (PEG ALG) Allo - EFP - day 4
J
K
Insulin
GLU
CD45
Nuclei
L
Insulin
CD3
B220
Nuclei
M
Insulin
CD31
MAC2
Nuclei
N
2000KDa FITC Dextran
Nuclei
O
2000KDa FITC Dextran
Nuclei

FIGURE 1 Conformal coating (CC) of pancreatic islets with polyethylene glycol functionalized with divinyl sulfone (PEG-dVS) and supplemented with alginate (ALG) does not provide immunoisolation. (A) Phase contrast images of naked and CC (5% PEG-dVS/0.8% MVG/DTT, PEG ALG) islets (scale bars, 100 μm). (B) Blood glucose of chemically induced diabetic B6 mice transplanted with 1000 IEQ naked (black, n = 5) or CC (PEG ALG) (orange, n = 7) islets from Balb/c mice under the kidney capsule (KD). CC and naked islets were transplanted 4 days after isolation and 2 days after encapsulation. (C) Confocal images of live (calcein, green)/dead (ethidium homodimer, red)/nuclei (Hoechst, blue) staining of naked and CC (PEG ALG) islets (scale bar, 100 μm). (D) Glucose-stimulated insulin release (GSIR) index of naked (black) versus CC (PEG ALG) (orange) islets from Balb/c mice 4 days after isolation and 2 days after encapsulation (2-3 replicates of 100 IEQ/condition, n = 2 experiments combined, $P = .45$). (E-G) H&E staining/light microscope images and immunofluorescence staining/confocal microscope images of CC (PEG ALG) grafts explanted after naked islet rejection occurred. E: H&E. F: insulin (green), glucagon (red), and nuclei (DAPI, blue). G: insulin (green), macrophages (mac2, red), and nuclei (DAPI, blue); scale bars 100 μm. (H-I) Blood glucose and allograft survival of diabetic B6 mice transplanted with 750 IEQ naked (black, n = 6) or CC (PEG ALG) (orange, n = 6) islets from Balb/c mice in the EFP using fibrin scaffolds.[13] (J-M) H&E staining/light microscope images and immunofluorescence staining/confocal microscope images of CC (PEG ALG) grafts explanted 4 days after implantation in the EFP site. J: H&E. Scale bar: 100 μm. K: insulin (green), glucagon (red), CD45 (cyan), and nuclei (DAPI, blue). L: insulin (green), T cells (CD3, red), B cells (B220, cyan), and nuclei (DAPI, blue. M: insulin (green), endothelial cells (CD31, red), macrophages (mac2, cyan), and nuclei (DAPI, blue). Scale bars: 50 μm. (N-O) Confocal images (maximum projection on y axis and orthogonal projection of ~5 μm-thick z-scan) of 2000 kDa FITC-labeled dextran entrapped in CC (PEG ALG) (N) or added to the CC islet media (O). Nuclei are counterstained with Hoechst (blue) showing pancreatic islets within capsules

complete and smooth conformal coatings around islets (Figure 2F-G) without compromising viability, as demonstrated by a comparable OCR of CC (PEG MG) islets and naked islets (Figure 2H). Unlike CC (PEG-dVS ALG), CC (PEG MG) was completely impermeable to high-molecular-weight dextran (Figure 2I). Despite lower permselectivity to 2 kDa dextran than to CC (PEG-dVS ALG), diffusion of lower-molecular-weight dextran through CC (PEG MG) was permitted with a diffusion kinetic that correlated with a dextran molecular weight (Figure 2J). In addition,, physiological insulin release of CC (PEG MG) islets was observed during a 0.1 ml/min dynamic glucose challenge (Figure 2K). These results suggest that biocompatibility properties of CC can be enhanced by using PEG-MAL MG as hydrogel for CC islets.

3.3 | PEG-MAL MG CC islets transplanted in the EFP site reverse diabetes long-term in murine allografts without immunosuppression

Following promising results of CC (PEG MG) in vitro, we evaluated whether CC (PEG MG) was immunoisolating and promoted long-term diabetes reversal after transplantation of fully MHC-mismatched allografts in mice without immunosuppression. We found that 75% of the diabetic B6 mice recipients of CC (PEG MG) Balb/c islets in the EFP reversed diabetes long-term (>100 days) without immunosuppression. In contrast, the majority (10/13) of mice exhibiting diabetes reversal with naked islets were rejected (Figure 3A-B, $P = .0097$). Long-term survivors (>100 days) had grafts explanted, and all mice returned to hyperglycemia, confirming that glucose homeostasis was dependent on CC graft function (Figure 3A). Histological and immunofluorescence evaluation of CC (PEG MG) grafts explanted >100 days after transplantation (Figure 3C) showed normal peripheral distribution of glucagon$^+$ α cells around insulin$^+$ β cells (Figure 3D), confirming long-term survival of CC (PEG MG) islets in the EFP site. It is notable that we found abundant graft revascularization as indicated by the presence of erythrocyte-containing CD31$^+$ blood vessels (Figure 3E and enlarged detail) close to CC islet. Despite abundant revascularization, we observed neither recruitment nor infiltration of T and B lymphocytes within CC grafts (Figure 3F), unlike what we observed with CC (PEG ALG) (Figure 1J-M). Moreover, minimal macrophage infiltration (Figure 3G) was also found, suggesting long-term biocompatibility of PEG MG hydrogel for CC. These results overall demonstrated that conformal coating using PEG MG as hydrogel composition is immunoisolating. Analysis of grafts that failed to maintain long-term euglycemia indicated that graft failure was not due to loss of immunoisolation, since T and B lymphocytes were not found within CC (PEG MG) capsules (Figure S1 A-D), unlike naked islet grafts (Figure S1 E-H). Immunostaining of CC (PEG MG) with PEG antibodies confirmed that coatings were intact (Figure 3H).

Given that the CC (PEG MG) islets remain void of significant lymphocytes infiltration, we next examined whether these capsules could alter allogeneic T cell responses. To address this, we performed an allogeneic (allo) MLR 14 days after transplantation. Diabetic B6 mice that received naked, CC (PEG ALG), or CC (PEG MG) Balb/c islets or from mice that received islet-free fibrin scaffolds were bled and lymphocytes stimulated in culture for 4 days with either PBL or SPLs of naive Balb/c mice. Histological analysis of CC (PEG ALG) grafts 4 days after implantation in the EFP site confirmed cell infiltrates (Figure 1J, H&E staining). Immune cell recruitment to the graft was observed (Figure 1K, CD45 staining), including T and B cells (Figure 1L, CD3 and B220 staining) and macrophages (Figure 1M, MAC2 staining) infiltration through the CC (PEG ALG) capsules, which could be mediating rejection of the CC grafts. Moreover, CC (PEG ALG) responders had more robust proliferation compared to the CC (PEG MG) mice. We observed a higher proliferation of CD8 cells from recipients of naked islets, but this difference did not reach statistical significance. A similar trend was also observed when CD8 cells were stimulated with PBLs from naive Balb/c (not shown). Peripheral blood CD8 T cells from all recipients proliferated in a manner similar to that of polyclonal anti-CD3 stimulation (Figure 4D). Phenotyping CD8$^+$ T cells from allo-MLR assays showed that proliferating CD8 responders from the naked and CC (PEG ALG) islet recipients are CD44 and Granzyme B$^+$, consistent with activation and cytotoxic phenotype (Figure 4E). Collectively, these data suggest that the CC (PEG MG) islets were not only void of penetrating lymphocytes but also failed to prime CD8 allo-responses, which likely contributed to their long-term acceptance following diabetes reversal compared to the CC (PEG ALG) or naked islets.

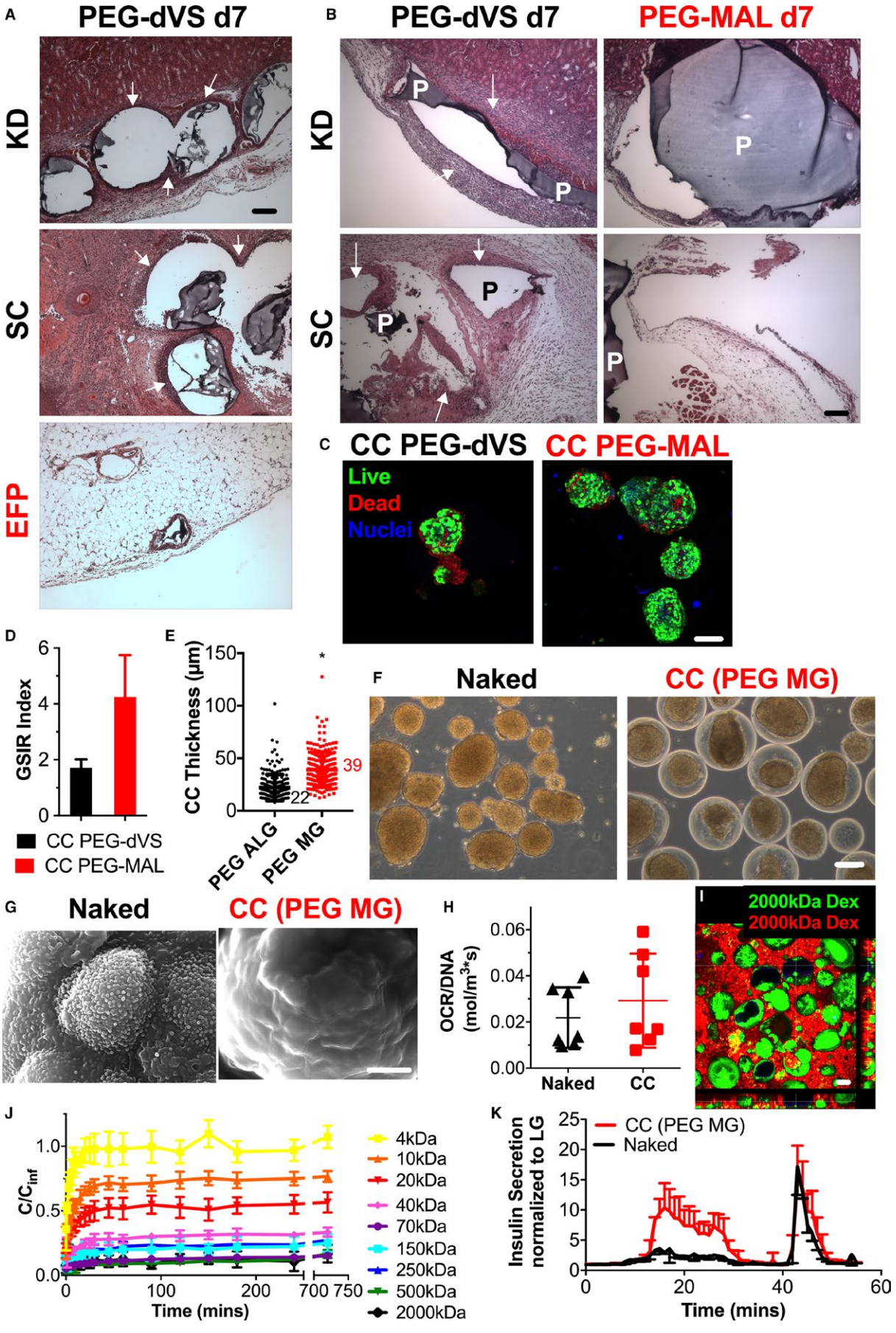
A
PEG-dVS d7
KD
SC
EFP
B
PEG-dVS d7
PEG-MAL d7
KD
SC
P
C
CC PEG-dVS
CC PEG-MAL
Live
Dead
Nuclei
D
GSIR Index
CC PEG-dVS
CC PEG-MAL
E
CC Thickness (μm)
22
39
PEG ALG
PEG MG
F
Naked
CC (PEG MG)
G
Naked
CC (PEG MG)
H
OCR/DNA (mol/m3*s)
Naked
CC
I
2000kDa Dex
2000kDa Dex
J
C/Cinf
Time (mins)
4kDa
10kDa
20kDa
40kDa
70kDa
150kDa
250kDa
500kDa
2000kDa
K
Insulin Secretion normalized to LG
CC (PEG MG)
Naked
Time (mins)

FIGURE 2 Refining the composition of CC to improve biocompatibility and immunoisolation. (A) H&E staining of islet-free 5% PEG-dVS capsules explanted 7 days after implantation at the kidney capsule site (KD), subcutaneous (SC) site, or epididymal fat pad (EFP) site of nondiabetic B6 mice (scale bar, 100 μm). Arrows show fibrosis. (B) H&E staining of islet-free 5% PEG-dVS (left) or 5% PEG-MAL (right) capsules explanted 7 days after implantation either at the KD (top panels) or SC (bottom panels) sites in nondiabetic B6 mice. P denotes the PEG capsules (scale bar, 100 μm). Combinations of site and PEG selected for studies with CC islets are indicated in red. Arrows show fibrosis. (C-D) Confocal microscope images of live (calcein AM, green)/dead (ethidium homodimer, red)/nuclei (Hoechst, blue) staining (C; scale bar, 100 μm) and GSIR Index (D) of CC (PEG-dVS, black) versus CC (PEG-MAL, red) islets from Lewis rats assessed 4 days after isolation and 2 days after encapsulation (2 replicates of 100 IEQ per condition) ($P = .24$). (E) Quantification of coating thickness of CC (PEG MG, red) and CC (PEG ALG, black) Balb/c islets. (F-G) Phase contrast (F; scale bar, 100 μm) and scanning electron microscopy (SEM) (G; scale bar, 2 μm) images of naked and CC (PEG MG) islets from Lewis rats. (H) Oxygen consumption rate (OCR) of naked (black) versus CC (PEG MG) (red) islets normalized to total DNA content ($P = .4$). (I) Confocal microscope image (orthogonal projections of ~5 μm thick z-scans) of 2000 kDa FITC-labeled-dextran entrapped within CC (PEG MG) capsules (green) and cultured in media containing 2000 kDa rhodamine-labeled dextran. Nuclei are counterstained with Hoechst (blue; scale bar 100 μm). (J) Permeability (indicated as instant concentration [C] normalized to the calculated concentration at equilibrium [C_{inf}]) of PEG MG islet-free 1-mm-diameter capsules to FITC-dextran molecules of selected molecular weights: 4 kDa (yellow), 10 kDa (orange), 20 kDa (red), 40 kDa (magenta), 70 kDa (purple), 150 kDa (cyan), 250 kDa (blue), 500 kDa (green), and 2000 kDa (black). (K) Perifusion assay (100 μL/min; 0-5 min 3 mM glucose; 6-25 minutes 11 mM glucose; 26-40 minutes 3 mM glucose; 41-45 minutes 30 mM KCl; 46-55 minutes 3 mM glucose) of naked (black) versus CC (PEG MG) (red) islets from Lewis rats assessed 4 days after isolation and 2 days after encapsulation (3 replicates of 100 IEQ/condition). *= $P < .05$

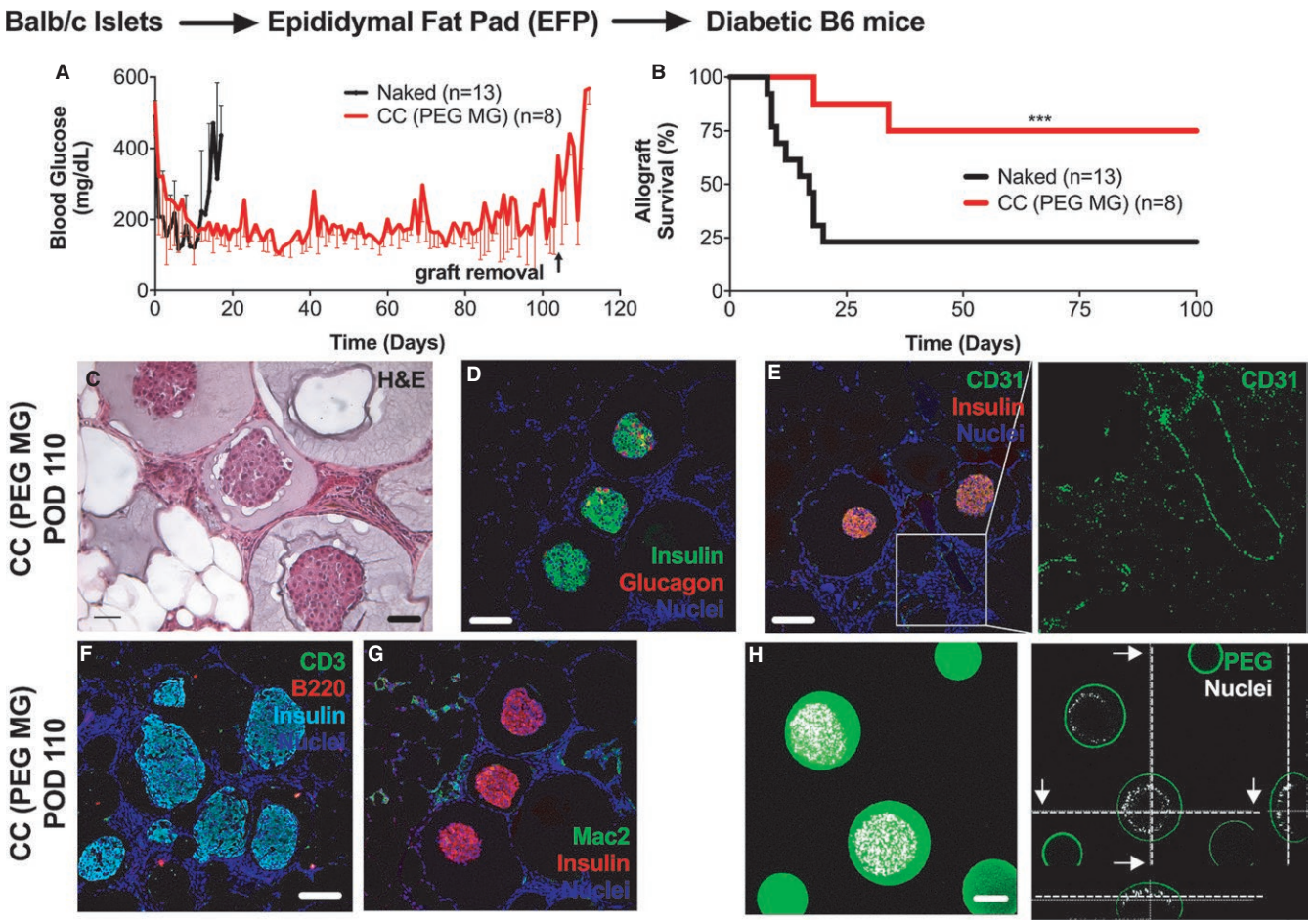

FIGURE 3 PEG-MAL MG conformal coated (CC) islets transplanted in the EFP site reverse diabetes long-term in murine allografts without immunosuppression. (A-B) Blood glucose of recipient mice (A) and survival (B) of 750-1000 IEQ naked (black, n = 13) or CC (PEG MG) (red, n = 8) islets from Balb/c mice transplanted into fully MHC-mismatched chemically induced diabetic B6 mice in the EFP site using fibrin scaffolds[13] without any immunosuppression. (C-H) Light microscope images (C) and immunofluorescent staining/confocal microscope images (D-G) of CC (PEG MG) allografts explanted >100 days after implantation in the EFP site. C: H&E. D: insulin (green), glucagon (red), and nuclei (DAPI, blue). E: vessel-lining endothelial cells (CD31, green), insulin (red), and nuclei (DAPI, blue). F: T cells (CD3, green), B cells (B220, red), insulin (cyan), and nuclei (DAPI, blue). G: macrophages (mac2, green), insulin (red), and nuclei (DAPI, blue). Scale bars, 100 μm. (H) PEG staining (green) and confocal imaging of CC (PEG MG) Balb/c islets. Nuclei are counterstained with DAPI (white). ***= $P < .001$

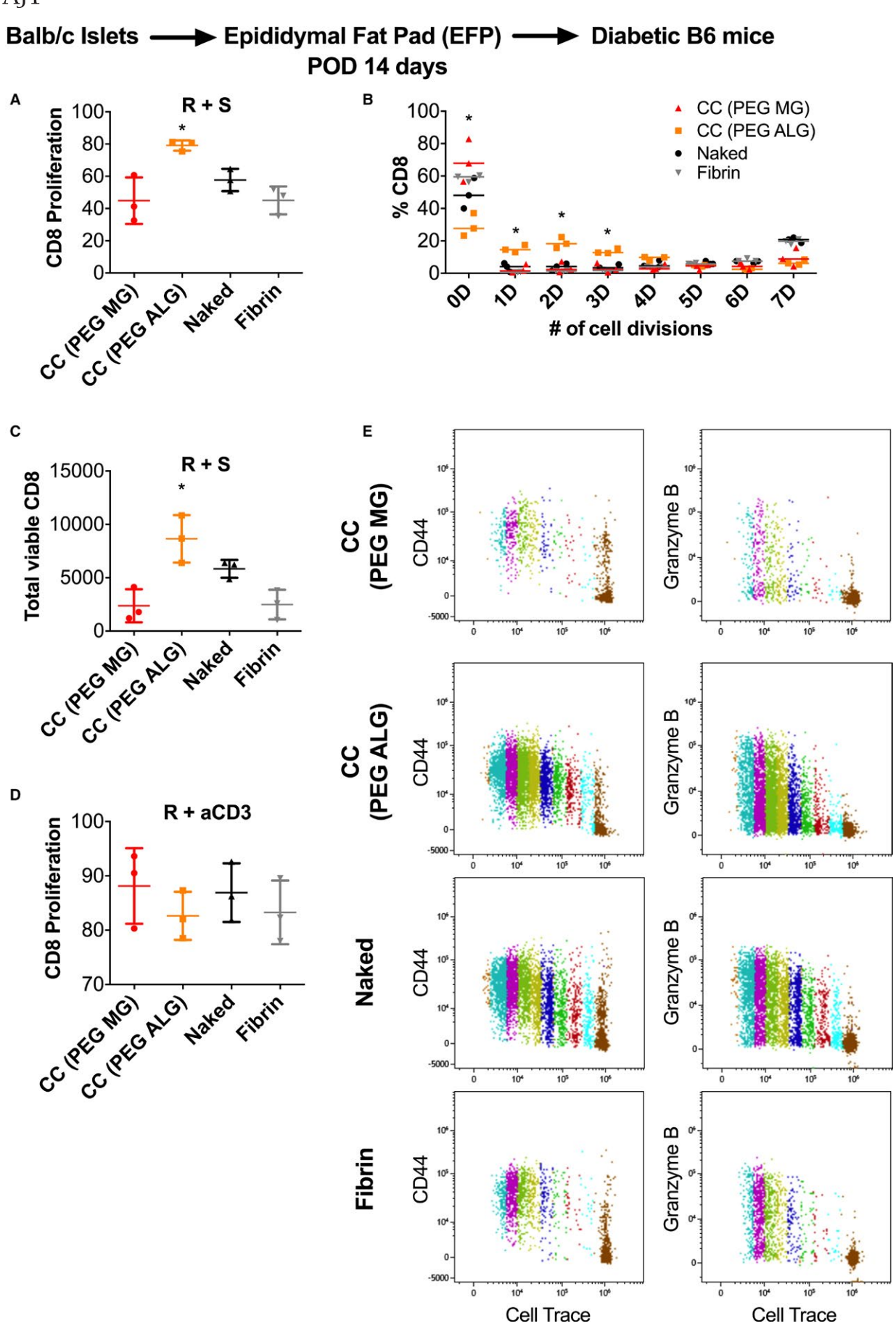
Balb/c Islets
Epididymal Fat Pad (EFP)
Diabetic B6 mice
POD 14 days
A
R + S
CD8 Proliferation
CC (PEG MG)
CC (PEG ALG)
Naked
Fibrin
B
% CD8
CC (PEG MG)
CC (PEG ALG)
Naked
Fibrin
0D
1D
2D
3D
4D
5D
6D
7D
# of cell divisions
C
R + S
Total viable CD8
D
R + aCD3
CD8 Proliferation
E
CC (PEG MG)
CC (PEG ALG)
Naked
Fibrin
CD44
Granzyme B
Cell Trace

FIGURE 4 Diabetic B6 mice transplanted with CC (PEG MG) Balb/c islets failed to prime recipient CD8 T cells. Peripheral blood lymphocytes (PBLs) from B6 recipient mice 14 days after transplantation of naked or CC (PEG ALG) or CC (PEG MG) islets or islet-free fibrin scaffolds (Fibrin). B6 recipient PBLs were co-cultured for 4 days with naive Balb/c splenocytes (R+ S_{SPL}) or stimulated with anti-CD3 (R+ αCD3). B6 recipient PBL activation was quantified by flow cytometry using CD44 and Granzyme B+ staining (activation) and cell trace dilution (proliferation). (A) Total percent (B) number of cell divisions, or (C) total number of viable CD8 B6 responders to allogeneic stimulation with Balb/c splenocytes. (D) Total proliferation of CD8 B6 responders to polyclonal anti-CD3 stimulation. (E) Dot plots showing cell trace dilution and CD44 or Granzyme B staining of CD8 cells after 4 days culture with naive Balb/c splenocytes. *= $P < .05$

3.4 | Decreased efficiency of diabetes reversal after transplantation of CC (PEG MG) islet allografts is dependent on host responses to CC islets but not to CC hydrogels

Although diabetes reversal was observed in some diabetic B6 mice transplanted with naked or CC (PEG MG) Balb/c islets, CC (PEG MG) islets overall did not reverse diabetes as efficiently as naked islets (Figure 5A). To investigate the mechanism underlying the suboptimal engraftment efficiency of CC allografts, we evaluated whether islets in PEG MG conformal capsules experienced loss of viability and/or GSIR function after encapsulation. We cultured naked and CC (PEG MG) Balb/c islets up to 14 days and found no significant difference in either viability or presence of reactive oxygen species (ROS) (Figure 5B) at 2, 7, and 14 days after encapsulation. GSIR index of CC (PEG MG) islets was significantly higher than that for naked islets both at day 2 and day 7 after encapsulation, while it was comparable at day 14 (Figure 5C). This suggested a beneficial effect of CC (PEG MG) on islet functionality and that reduced diabetes reversal rate of CC versus naked islets was not due to loss of viability or function. Therefore, we examined the host responses to CC (PEG MG) after transplantation. Because host responses may be mediated by PEG MG biomaterials themselves (biocompatibility) or by bioactive molecules secreted by CC (PEG MG) islets, we co-transplanted naked syngeneic B6 islets and cell-free empty PEG MG capsules into diabetic B6 recipient mice (750 IEQ/mouse). We saw no difference in diabetes reversal efficiency (Figure 5D) and long-term blood glucose control (Figure 5E) compared to naked islets or CC islets (n = 4 per condition; $P = .127$ and $P = .18$). Histological evaluation of CC (PEG MG) grafts 100 days after implantation in syngeneic recipients confirmed lack of macrophage accumulation and maintenance of islet architecture (Figure 5F). These results suggested that host immune responses to PEG MG hydrogels themselves were not the underlying cause of the reduced graft reversal efficiency of CC (PEG MG) islets.

Next, we examined whether secretion of proinflammatory and anti-inflammatory cytokines from CC (PEG MG) islets during in vitro culture were affected by coatings and whether this was time dependent. We found that interferon γ (IFNγ) (Figure 5L), IL-1β (Figure 5M), IL-13 (Figure 5N), and MIP1α (Figure 5O) proinflammatory cytokine secretion was increased in CC compared to naked islets. IL-10 (Figure 5P) and IL-4 (Figure 5Q) anti-inflammatory and Th2 cytokines secretion was reduced in CC compared to naked islets. In contrast, tumor necrosis factor α (TNFα) (Figure 5G), MCP-1 (Figure 5H), IL1α (Figure 5I), IL-6 (Figure 5J), and IL-2 (Figure 5K) proinflammatory cytokine secretion was comparable or even reduced in CC compared to naked islets. Because the same mouse strain was used as recipient for allogeneic (Figure 5A) and syngeneic (Figure 5D) islets, these results suggest that host responses to CC (PEG MG) islets could be heightened in the presence of allogeneic islets in CC hydrogels, which in a portion of the mice prevented engraftment and diabetes reversal after transplantation of CC allogeneic, but not CC syngeneic islets.

Next, we analyzed the grafts 4 days after transplantation by immunohistochemistry to evaluate the presence of leukocytes at the transplant site. CC islets were found intact inside capsules and void of T cells, B cells, or macrophages within the capsules, which was in stark contrast to the transplanted naked islets (Figure 6A). However, we observed the presence of immune cells to the graft periphery of CC (PEG MG) islets. Quantification and phenotypic characterization of these infiltrates confirmed that higher numbers of $CD45^+$ cells were present in both naked and CC islet grafts (Figure 6B) and higher numbers of macrophages in CC islet grafts (Figure 6D) compared to islet-free fibrin grafts. No differences in total number and relative proportions of T cells and other antigen-presenting cell subtypes were found. However, among the $CD8^+$ T cells infiltrating CC grafts, we found higher proportions of proliferating cells with an effector phenotype ($CD44^+$ $CD127^-$) and fewer proportions of naive cells ($CD44^-$ $CD127^-$ $CD62L^+$) (Figure 6C). Therefore, we concluded that although the CC (PEG MG) prevent immune cell infiltrate inside the capsules, the local microenvironment around the capsules recruits leukocytes to the graft site and may contribute to the suboptimal diabetes reversal we observed after transplantation of CC (PEG MG) islets.

4 | DISCUSSION

Our overall goal is to develop an encapsulation platform that allows islet transplantation without immunosuppression, extending its applicability to a larger number of patients with T1D. Conformal coating encapsulation addresses some critical issues that may have led to clinical failure of traditional encapsulation protocols using traditional microcapsules in the IP site. Specifically, CC capsules allow transplantation of curative doses of encapsulated islets in confined well-vascularized sites, which we previously demonstrated to be superior to the IP site.[14] Here, we built on our previous work that established the novel procedure for conformal coating with PEG using suboptimal hydrogels. We found that those do not confer immunoisolation to islet allografts. In addition, that study was performed in nonclinically relevant transplant sites. In this report, we refined the

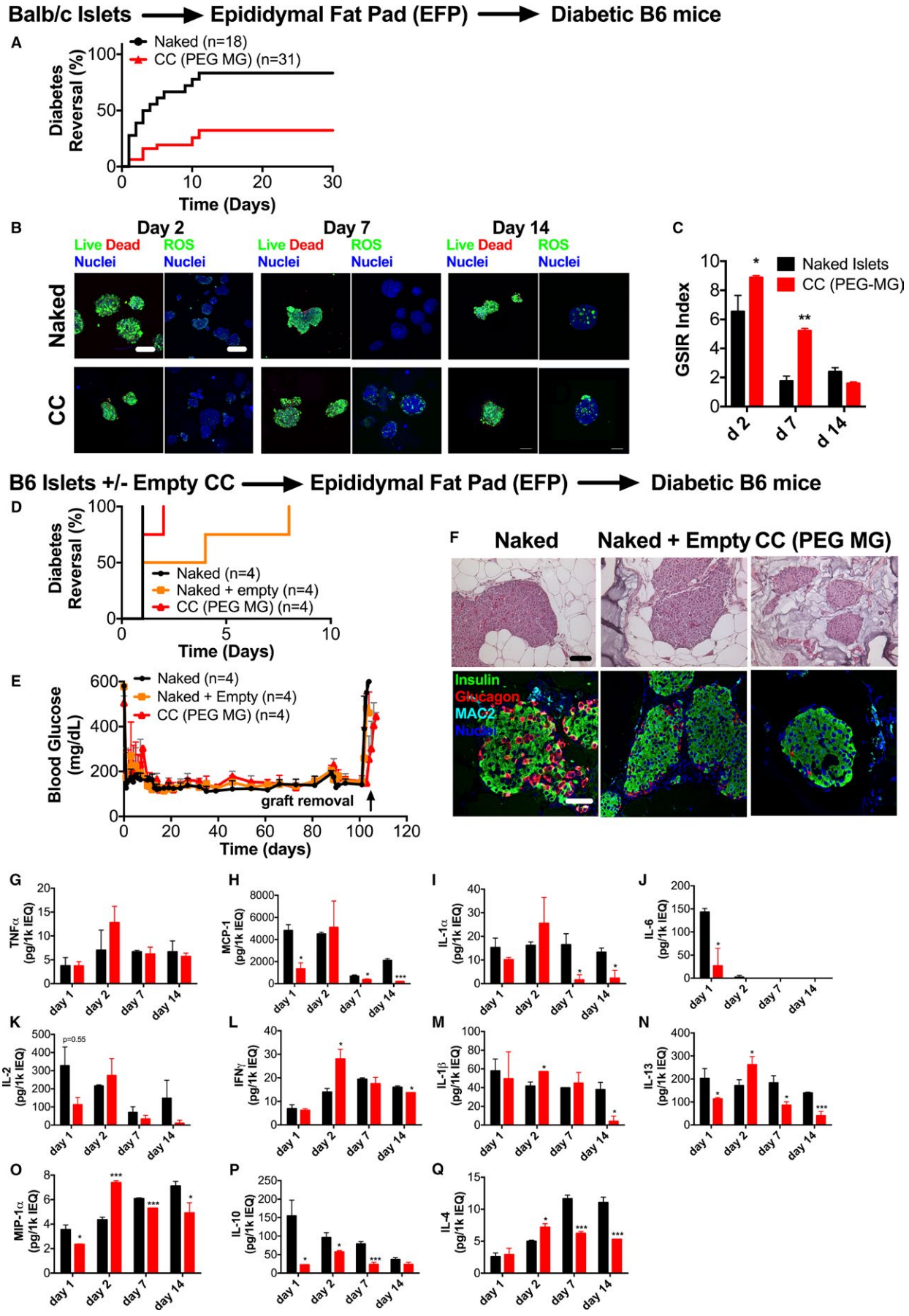
Balb/c Islets → Epididymal Fat Pad (EFP) → Diabetic B6 mice
A
Naked (n=18)
CC (PEG MG) (n=31)
Diabetes Reversal (%)
Time (Days)
B
Day 2
Day 7
Day 14
Live Dead Nuclei
ROS Nuclei
Naked
CC
C
Naked Islets
CC (PEG-MG)
GSIR Index
d 2
d 7
d 14
B6 Islets +/- Empty CC → Epididymal Fat Pad (EFP) → Diabetic B6 mice
D
Naked (n=4)
Naked + empty (n=4)
CC (PEG MG) (n=4)
Diabetes Reversal (%)
Time (Days)
E
Naked (n=4)
Naked + Empty (n=4)
CC (PEG MG) (n=4)
Blood Glucose (mg/dL)
graft removal
Time (days)
F
Naked
Naked + Empty CC (PEG MG)
Insulin
Glucagon
MAC2
Nuclei
G
TNFα (pg/1k IEQ)
H
MCP-1 (pg/1k IEQ)
I
IL-1α (pg/1k IEQ)
J
IL-6 (pg/1k IEQ)
K
IL-2 (pg/1k IEQ)
p=0.55
L
IFNγ (pg/1k IEQ)
M
IL-1β (pg/1k IEQ)
N
IL-13 (pg/1k IEQ)
O
MIP-1α (pg/1k IEQ)
P
IL-10 (pg/1k IEQ)
Q
IL-4 (pg/1k IEQ)
day 1
day 2
day 7
day 14

FIGURE 5 Decreased efficiency of diabetes reversal after transplantation of CC (PEG MG) islet allografts is dependent on host responses to CC islets but not to CC hydrogels. (A) Percentage of chemically induced diabetic B6 mice transplanted with 750-1000 IEQ naked (black, n = 18) or CC (PEG MG) (red, n = 31) islets from Balb/c mice that reversed diabetes after transplantation in the EFP site using fibrin scaffolds [13] (***=$P < .0001$). (B) Confocal microscope images of live (calcein AM, green)/dead (ethidium homodimer, red)/nuclei (Hoechst, blue) staining (left) and reactive oxygen species (ROS, green)/nuclei (Hoechst, blue) staining (right) of naked (top panels) versus CC (PEG MG) (bottom panels) islets from Lewis rats assessed 2, 7, and 14 days after encapsulation (4, 9, and 16 days after isolation) and cultured in vitro (scale bars, 100 μm). (C) GSIR index of naked (black) versus CC (PEG MG) (red) islets from Lewis rats evaluated 2, 7, and 14 days after encapsulation (4, 9, and 16 days after isolation, 3 replicates of 100 IEQ per condition) (Index naked vs. CC PEG MG: day 2 $P = .0099$, day 7 $P = .014$, day 14 $P = .4064$). (D-F) Percentage of diabetes reversal (D), blood glucose (E), and histological analysis (F) of chemically induced diabetic B6 mice transplanted with 750 IEQ naked islets (naked, black, n = 4) or CC (PEG MG) islets (red, n = 4) or naked islets with islet-free empty PEG MG capsules (Naked + empty, orange, n = 4) from B6 mice in the EFP site using fibrin scaffolds.[13] F: H&E staining (top) and immunofluorescent staining/confocal imaging (bottom): insulin (green), glucagon (red), macrophages (Mac2, cyan), nuclei (DAPI, blue). Scale bars, 50μm. (G-Q) Secretion of proinflammatory TNFα (G), MCP-1 (H), IL1α (I), IL-6 (J), IL-2 (K), IFNγ (L), IL-1β (M), IL-13 (N), MIP1α (O), and antiinflammatory IL-10 (P) and IL-4 (Q) cytokines by naked (black) versus CC (PEG MG) (red) islets from Lewis rats cultured in vitro and assessed 1, 2, 7, and 14 days after encapsulation (4, 9, and 16 days after isolation). TNFα, tumor necrosis factor alpha; MIP-1α, macrophage inflammatory protein alpha (CCL3); IFNγ, interferon gamma; MCP-1, monocyte chemoattractant protein (CCL2) (N = 3 per time point. *= $P < .05$; **= $P < .01$; ***= $P < .0001$)

composition of CC hydrogels and showed that CC using PEG hydrogels allows immunoisolation of islet allografts in clinically applicable confined and well-vascularized sites with high potential for clinical translation.

We previously reported the design of the encapsulation device and the properties of the CC hydrogels, which was based on PEG hydrogels, supplemented with ALG to increase the pre-polymer viscosity and modulate the coating permeability.[14] CC (PEG ALG) showed promising results in vitro and in vivo in syngeneic islet transplant models at the nonclinically relevant but most common transplant site in mice, the KD. Here, we demonstrated that such combination of composition (PEG ALG) and transplant site (KD) did not allow long-term diabetes reversal after transplantation of fully MHC-mismatched CC islet allografts in mice. This was due in part to poor immunoisolation properties (ie, the high microporosity of PEG ALG capsules and increased allogeneic T cells responses) and in part to the suboptimal biocompatibility of PEG-dVS in the KD site. Most previous work on encapsulated islets was done using the IP as transplant site because of volume limitations imposed by the large diameter of traditional capsules, with no previous studies evaluating the host reactivity to microencapsulated islets in the KD site and other confined sites. Previous studies demonstrated that in the IP and the SC site, larger capsules displayed the highest biocompatibility.[19] This study using CC islets complements our previous studies with CC and traditional alginate microencapsulated islets, comparing graft outcomes in different transplantation sites and for different capsule hydrogel compositions. Although in our report of the previous study we found that suboptimal biocompatibility of PEG-dVS ALG in the KD site did not impair islet graft functionality in syngeneic grafts, here we found that the reaction to the empty PEG-dVS ALG capsules in the KD site combined with suboptimal immunoisolating properties of PEG-dVS ALG hydrogels did not allow long-term survival of CC (PEG-dVS ALG) allografts. We have replaced PEG-dVS with a less-reactive PEG-MAL and moved transplant to the vascularized EFP site, which minimizes host reactions to PEG hydrogels while improving the outcome of both naked[13] and encapsulated islet grafts[14] in mice. To address the issue of poor immunoisolation of PEG ALG hydrogels due to their microporosity we found that recapitulating the composition of the islet-like ECM using MG increased immunoisolation properties of CC hydrogels without compromising islet functionality. These results are in agreement with those of previous reports showing that the islet-like ECM provides a barrier to leukocyte infiltration in pancreatic islets[18] and is beneficial to islet function.[20] Using MG as an additive to PEG allowed diabetes reversal and long-term survival of fully MHC-mismatched CC (PEG MG) islet allografts in some mice, without any immunosuppression compared to the same dose of naked islets that was required for diabetes reversal. Improved immunoisolation was associated with a lack of allogeneic priming with transplanted CC (PEG MG) islets, which likely contributed to long-term islet graft survival in mice.

One drawback of the current CC composition CC (PEG MG) is the suboptimal rate of diabetes reversal we observed after transplantation of allogeneic CC islets in diabetic mice when no immunosuppression is used. Recruitment and accumulation of both B and T cells in CC allografts that failed to reverse diabetes, and recruitment and accumulation of effector CD8 T cells in CC allografts as early as 4 days after transplantation around but not inside conformal capsules, suggest that indirect effects of immune cells might prevent islet engraftment in a portion of the transplanted animals. Because the reduced engraftment efficiency of CC islets was seen only in allogeneic and not in syngeneic recipients, it is likely that indirect immune responses in the microenvironment triggered by the presence of Th1 cytokine release by CC islets at the transplantation site played a critical role in determining outcomes of CC allografts. This conclusion is supported by the fact that 100% diabetes reversal was observed after transplantation of syngeneic CC islets. Therefore, short-term systemic or local treatment within the transplant site and/or the transplantation scaffolds with immunomodulatory drugs that block inflammatory cytokines from encapsulated islets at the time of transplantation will likely improve diabetes reversal efficiency of CC allografts. Drugs targeting the specific pathways affected (IL1-β: anakinra; and mammalian target of rapamycin [mTOR] and calcineurin inhibitors: sirolimus and tacrolimus) are clinically available and currently used in clinical islet transplantation. A further option to improve diabetes reversal efficiency would be to increase the islet dose per recipient, which may be feasible due to recent advances in generating inexhaustible sources of insulin-secreting cell products from stem cells.[21, 22]

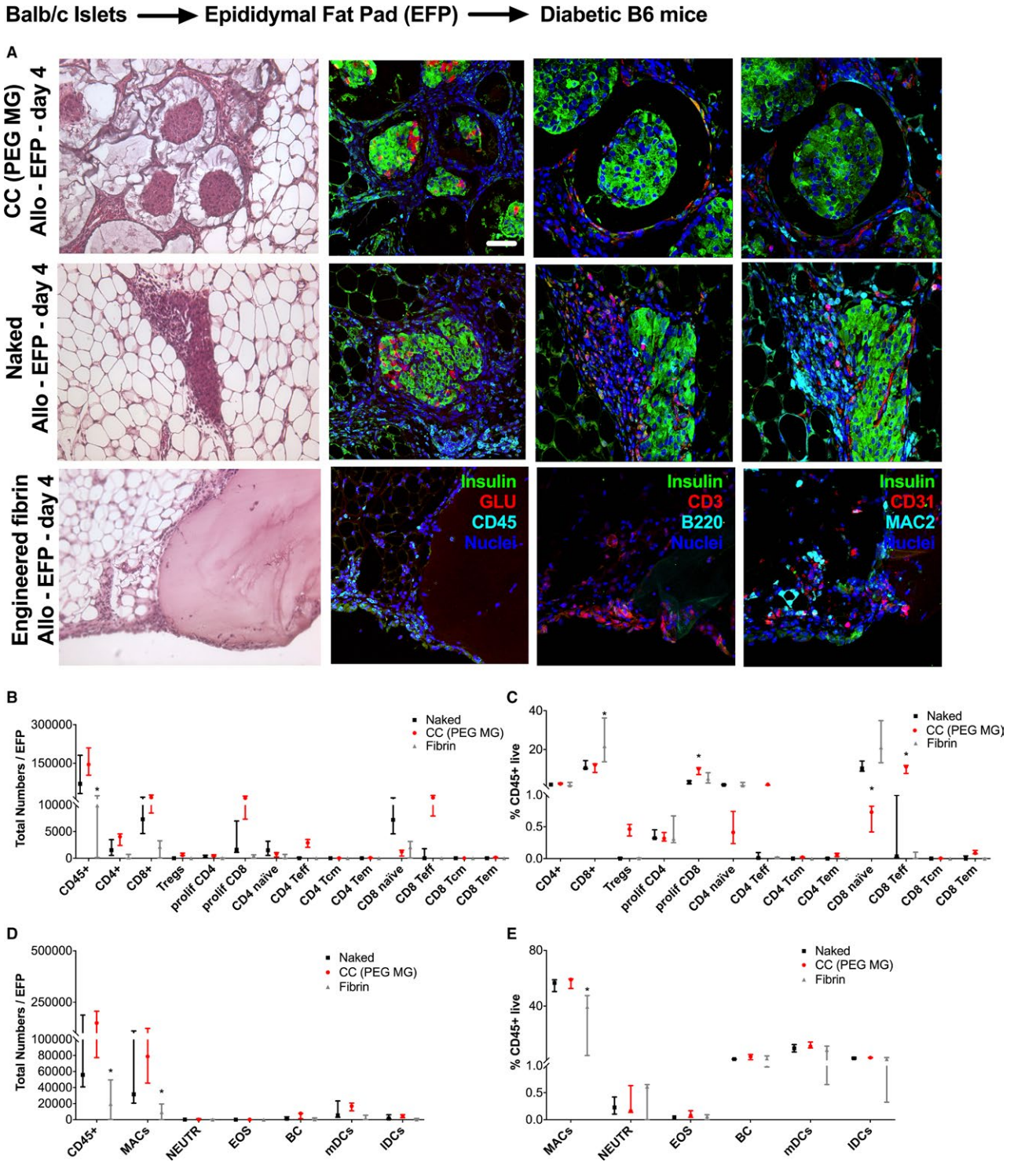

FIGURE 6 Analysis of CC (PEG MG) islet allografts 4 days after transplantation in the EFP site of diabetic mice. (A) H&E staining/light microscope images (left column) and immunofluorescence staining/confocal microscope images (right columns) of CC (PEG MG) (top row), naked (middle row), and islet-free fibrin (bottom row) grafts explanted 4 days after implantation in the EFP site. Left column: H&E. Scale bar, 100 μm. Second column: insulin (green), glucagon (red), CD45 (cyan), and nuclei (DAPI, blue). Third column: insulin (green), T cells (CD3, red), B cells (B220, cyan), and nuclei (DAPI, blue). Right column: insulin (green), endothelial cells (CD31, red), macrophages (Mac2, cyan), and nuclei (DAPI, blue). Scale bars: 50 μm. (B-E) Quantification of T cells (B-C) and of antigen-presenting cells (D-E) from EFP containing CC (PEG MG) (red), naked (black), and islet-free fibrin (gray) grafts explanted 4 days after implantation by flow cytometry. Both total cell numbers (B, D) and percentage of $CD45^+$ cells are shown. T_{regs} ($CD4^+$ $FoxP3^+$ $CD25^{hi}$), proliferating $CD4^+$ and $CD8^+$ T cells ($Ki\text{-}67^+$), T naive ($CD44^-$ $CD127^-$ $CD62L^+$), T effectors ($CD44^+$ $CD127^-$), T central memory (T_{CM}) ($CD44^+$ $CD127^+$ $CD62L^+$), and T effector memory (T_{EM}) ($CD44^+$ $CD127^+$ $CD62L^-$). Macrophages (MAC, $CD11b^+$ $F4/80^+$ $B220^-$), neutrophils (NEUTR, $CD11b^+$ $GR\text{-}1^+$), eosinophils (EOS, $CD11b^+$ $GR\text{-}1^+$ $F4/80^+$), B cells (BC, $CD11b^-$ $F4/80^-$ $B220^+$), myeloid dendritic cells (mDCs, $CD11b^+$ $CD11c^+$ I-A/I-E^+), and lymphoid dendritic cells (lDCs, $CD11b^-$ $CD11c^+$ I-A/I-E^+). *= $P < .05$

Despite the challenge in diabetes reversal, we demonstrated that conformal coating encapsulation is a valid platform to allow islet allotransplantation without immunosuppression. The main advantage of conformal coating encapsulation over other encapsulation strategies is the reduced graft volume, allowing CC islets to be transplanted into any site. This includes the intrahepatic site, biohybrid and/or pre-vascularized devices [23-27] and the biologic scaffold in the omental pouch (OP) site,[26] which are currently explored in a very promising human clinical trial with naked allogeneic islets and chronic immunosuppression (NCT02213003).

ACKNOWLEDGMENTS

The authors are grateful to Dr. C. Fraker, DRI, for his help with OCR in vitro assessments; to Dr. M. Abreu for her help with immunostaining optimization and confocal imaging; to Drs. Diana Velluto and Maria Abreu for reading the manuscript and providing feedback; to the personnel of the DRI Preclinical Cell Processing and Translational Models Core for their help with islet isolation, transplantation, and management of diabetic mice; to the DRI Imaging Core for providing expertise on confocal imaging; and to the DRI Histology core headed by Kevin Johnson for his help with histological processing of all samples. Funding was provided by philanthropic funds from the Diabetes Research Institute Foundation, grants from the Juvenile Diabetes Research Foundation (grant #17-2001-268, 17-2010-5, and 17-2012-361), the National Institutes of Health (grant #DK109929), the Fondazione Tronchetti Provera, and the Fondazione IRCCS Ca' Granda Ospedale Maggiore Policlinico.

DISCLOSURE

The authors of this manuscript have conflicts of interest to disclose as described by the *American Journal of Transplantation*. A.A.T. and J.A.H. are co-inventors of intellectual property used in the study and may gain royalties from future commercialization of the technology licensed to Converge Biotech Inc. C.R. is a member of the scientific advisory board and stock option holder in Converge Biotech, licensee of some of the intellectual property used in this study. A.A.T., V.M., and R.D.M. are stock option holders in Converge Biotech. The other authors have no conflicts of interest to disclose.

AUTHOR CONTRIBUTIONS

V.M. wrote the manuscript and generated data. C.V. generated data and contributed to the discussion. A.L.B. and R.D.M. generated data, reviewed/edited the manuscript, and contributed to the discussion. L.M. generated data. Y.T., C.R., and J.A.H. contributed to the discussion. A.A.T. designed the research and wrote the manuscript.

ORCID

Alice A Tomei http://orcid.org/0000-0002-5059-6303

REFERENCES

1. Shapiro AM, Lakey JR, Ryan EA, et al. Islet transplantation in seven patients with type 1 diabetes mellitus using a glucocorticoid-free immunosuppressive regimen. *N Engl J Med*. 2000;343(4):230-238.
2. Bruni A, Gala-Lopez B, Pepper AR, Abualhassan NS, Shapiro AJ. Islet cell transplantation for the treatment of type 1 diabetes: recent advances and future challenges. *Diabetes Metab Syndr Obes*. 2014;7:211-223.
3. Gibly RF, Graham JG, Luo X, Lowe WL Jr, Hering BJ, Shea LD. Advancing islet transplantation: from engraftment to the immune response. *Diabetologia*. 2011;54(10):2494-2505.
4. Cantarelli E, Piemonti L. Alternative transplantation sites for pancreatic islet grafts. *Curr DiabRep*. 2011;11(5):364-374.
5. Basta G, Calafiore R. Immunoisolation of pancreatic islet grafts with no recipient's immunosuppression: actual and future perspectives. *Curr DiabRep*. 2011;11(5):384-391.
6. O'Sullivan ES, Vegas A, Anderson DG, Weir GC. Islets transplanted in immunoisolation devices: a review of the progress and the challenges that remain. *Endocr Rev*. 2011;32(6):827-844.
7. Tuch BE, Keogh GW, Williams LJ, et al. Safety and viability of microencapsulated human islets transplanted into diabetic humans. *Diabetes Care*. 2009;32(10):1887-1889.
8. Desai T, Shea LD. Advances in islet encapsulation technologies. *Nat Rev Drug Discovery*. 2017;16(5):338-350.
9. Weir GC. Islet encapsulation: advances and obstacles. *Diabetologia*. 2013;56(7):1458-1461.
10. Scharp DW, Marchetti P. Encapsulated islets for diabetes therapy: history, current progress, and critical issues requiring solution. *Adv Drug Deliv Rev*. 2014;67–68:35-73.
11. Calafiore R, Basta G. Clinical application of microencapsulated islets: actual prospectives on progress and challenges. *Adv Drug Deliv Rev*. 2014;67–68:84-92.
12. Rabanel JM, Banquy X, Zouaoui H, Mokhtar M, Hildgen P. Progress technology in microencapsulation methods for cell therapy. *Biotechnol Prog*. 2009;25(4):946-963.
13. Najjar M, Manzoli V, Villa C, et al. Fibrin gels engineered with pro-angiogenic growth factors promote engraftment of pancreatic islets in extrahepatic sites in mice. *Biotechnol Bioeng*. 2015;112:1916-1926.
14. Villa C, Manzoli V, Abreu MM, et al. Effects of composition of alginate-polyethylene glycol microcapsules and transplant site on encapsulated islet graft outcomes in mice. *Transplantation*. 2017;101:1025-1035.
15. Tomei AA, Manzoli V, Fraker CA, et al. Device design and materials optimization of conformal coating for islets of Langerhans. *Proc Natl Acad Sci USA*. 2014;111(29):10514-10519.
16. Orr JS, Kennedy AJ, Hasty AH. Isolation of adipose tissue immune cells. *J Vis Exp*. 2013;75:e50707. https://doi.org/10.3791/50707
17. Phelps EA, Enemchukwu NO, Fiore VF, et al. Maleimide cross-linked bioactive PEG hydrogel exhibits improved reaction kinetics and cross-linking for cell encapsulation and in situ delivery. *Adv Mater*. 2012;24(1):64-70, 2.
18. Korpos E, Kadri N, Kappelhoff R, et al. The peri-islet basement membrane, a barrier to infiltrating leukocytes in type 1 diabetes in mouse and human. *Diabetes*. 2013;62(2):531-542.
19. Veiseh O, Doloff JC, Ma M, et al. Size- and shape-dependent foreign body immune response to materials implanted in rodents and non-human primates. *Nat Mater*. 2015;14(6):643-651.
20. Llacua A, de Haan BJ, Smink SA, de Vos P. Extracellular matrix components supporting human islet function in alginate-based immunoprotective microcapsules for treatment of diabetes. *J Biomed Mater Res, Part A*. 2016;104(7):1788-1796.
21. Pagliuca FW, Millman JR, Gurtler M, et al. Generation of functional human pancreatic beta cells in vitro. *Cell*. 2014;159(2):428-439.

22. Rezania A, Bruin JE, Arora P, et al. Reversal of diabetes with insulin-producing cells derived in vitro from human pluripotent stem cells. *Nat Biotechnol*. 2014;32(11):1121-1133.
23. Pepper AR, Pawlick R, Gala-Lopez B, et al. Diabetes is reversed in a murine model by marginal mass syngeneic islet transplantation using a subcutaneous cell pouch device. *Transplantation*. 2015;99(11):2294-2300.
24. Desai T, Shea LD. Advances in islet encapsulation technologies. *Nat Rev Drug Discovery*. 2016;16:338-350.
25. Krishnan R, Alexander M, Robles L, Foster CE 3rd, Lakey JR. Islet and stem cell encapsulation for clinical transplantation. *Rev Diabet Stud*. 2014;11(1):84-101.
26. Berman DM, Molano RD, Fotino C, et al. Bioengineering the endocrine pancreas: intraomental islet transplantation within a biologic resorbable scaffold. *Diabetes*. 2016;65:1350-1361.
27. Juang JH, Bonner-Weir S, Ogawa Y, Vacanti JP, Weir GC. Outcome of subcutaneous islet transplantation improved by polymer device. *Transplantation*. 1996;61(11):1557-1561.

SUPPORTING INFORMATION

Additional Supporting Information may be found online in the supporting information tab for this article.

How to cite this article: Manzoli V, Villa C, Bayer AL, et al. Immunoisolation of murine islet allografts in vascularized sites through conformal coating with polyethylene glycol. *Am J Transplant*. 2017;00:1–14. https://doi.org/10.1111/ajt.14547